Statistical mechanics of patterned inhomogeneous fluid phenomena

1999 J. Phys.: Condens. Matter 11 629

(http://iopscience.iop.org/0953-8984/11/3/004)

J. Phys.: Condens. Matter **11** (1999) 629–643. Printed in the UK PII: S0953-8984(99)96974-6

Statistical mechanics of patterned inhomogeneous fluid phenomena

J R Henderson

Department of Physics and Astronomy, University of Leeds, Leeds LS2 9JT, UK

Received 25 August 1998 , in final form 21 October 1998

Abstract. A statistical mechanical framework is developed for generating exact results describing patterned inhomogeneous fluid phenomena. Generic models of patterning and corrugation are discussed, with specific choices of the pattern field invoked to provide a set of illustrative examples. Virial theorems are derived and complications inherent in the virial route to the surface tension of patterned interfaces are highlighted. A variety of compressibility sum rules describe new physics arising from the extended phase space available to patterned fluids. Applications include the wetting of patterned substrates and the solvation of patterned porous media.

1. Introduction

The number of exact results that are readily generated from equilibrium statistical mechanics grows rapidly with the complexity of the system; see e.g. [1]. Complex fluids are especially suited to rigorous theoretical analysis because fluids flow and thus adopt equilibrium states. Complexity of equilibrium many-body systems can be defined in terms of the number of relevant thermodynamic fields that form the axes of the statistical thermodynamical phase space containing the phenomena of interest. The set of relevant thermodynamic fields depends on the choice of statistical mechanical ensemble; i.e. the quantities that are to be regarded as under independent control. The key property of a thermodynamic field is that it adopts an identical value throughout all phases in equilibrium with one another. Temperature (T) and chemical potential (μ_i, one for each molecular species) form the set of bulk thermodynamic fields appropriate to the grand canonical ensemble. However, to fully characterize the phase space of molecular systems it is often appropriate to enlarge this set. For example, liquid-crystalline states of matter are usefully thought of as belonging to a phase space containing at least one quantity describing the shape of the molecule; say, the length-to-breadth ratio [2]. If at isotropic–nematic phase coexistence the geometric parameter is the same in both phases, as is appropriate to thermotropics (but not necessarily lyotropic surfactant systems), then it represents a perfectly well-defined thermodynamic field, that in addition is specified directly by the Hamiltonian.

Inhomogeneous fluids involve additional degrees of freedom, controlling phenomena such as wetting, orientational wetting, capillary condensation and competitive adsorption. Thus, inhomogeneous fluid phenomena are more complex than bulk phenomena; the relevant phase space is bigger. The important physics is captured by incorporating the additional thermodynamic fields as parameters within the one-body term in the Hamiltonian (formally, a translationally invariant Hamiltonian cannot describe inhomogeneous equilibrium states, so a one-body field must included, [3]). For example, the physics of wetting is described by models

0953-8984/99/030629+15$19.50

where the substrate (spectator phase) is replaced by an external field or wall, with the repulsive wall–fluid interaction defining the position of the interface and the attractive wall–fluid well depth (ϵ_w) defining the key wetting thermodynamic field. When the wall is in contact with a fluid at bulk two-phase coexistence, variation of ϵ_w by amounts of order k_BT (where k_B denotes Boltzmann's constant) induces interfacial phase transitions known as wetting transitions.

It is always possible to use an ensemble whose thermodynamic potential is a convex function of the set of relevant thermodynamic fields, alone, [4]. In this case, the second law defines a set of densities conjugate to each field. For example, the basic model of wetting described above yields

$$\mathrm{d}\gamma(T,\mu,\epsilon_w) = -s\,\mathrm{d}T - \Gamma\,\mathrm{d}\mu - \Theta\,\mathrm{d}\epsilon_w \tag{1}$$

where γ denotes the surface excess grand potential per unit surface area (A), s is the surface excess entropy per unit area, and Γ and Θ are the adsorption and surface density, respectively. Each of the fields is a parameter within the Boltzmann probability factor that defines the thermodynamic potential,

$$\exp\{-(U - \epsilon_w\hat{N}_1 - \mu\hat{N})/k_BT\} \tag{2}$$

where U denotes the many-body Hamiltonian, and the external-field term and the chemical potential contribution involve the following fluctuating one-body densities:

$$\hat{N}_1 \equiv -\int \mathrm{d}\boldsymbol{r}\;\hat{\rho}(\boldsymbol{r})v(\boldsymbol{r}) \tag{3}$$

$$\hat{N} \equiv \int \mathrm{d}\boldsymbol{r}\;\hat{\rho}(\boldsymbol{r}) \tag{4}$$

$$\hat{\rho}(\boldsymbol{r}) \equiv \sum_i \delta(\boldsymbol{r} - \boldsymbol{r}_i). \tag{5}$$

In equation (3) I have assumed a model in which the external field is of the form

$$v^{ext}(\boldsymbol{r}) \equiv \epsilon_w v(\boldsymbol{r}) \tag{6}$$

but of course one could equally well define $v(\boldsymbol{r})$ to be just an attractive contribution to the wall–fluid interaction. From the definition of the grand potential (Ω) in terms of the grand canonical partition function it is immediate that

$$-\frac{\partial\Omega}{\partial\mu} = \langle\hat{N}\rangle \tag{7}$$

$$-\frac{\partial\Omega}{\partial\epsilon_w} = \langle\hat{N}_1\rangle \equiv \Theta A \tag{8}$$

where the last equivalence makes direct contact with the second law (1). Further derivatives of the potential with respect to the thermodynamic fields generate a set of compressibilities:

$$-k_BT\frac{\partial^2\Omega}{\partial\mu^2} = \langle(\hat{N} - \langle\hat{N}\rangle)^2\rangle \tag{9}$$

$$-k_BT\frac{\partial^2\Omega}{\partial\epsilon_w^2} = \langle(\hat{N}_1 - \langle\hat{N}_1\rangle)^2\rangle \tag{10}$$

$$-k_BT\frac{\partial^2\Omega}{\partial\mu\,\partial\epsilon_w} = \langle(\hat{N} - \langle\hat{N}\rangle)(\hat{N}_1 - \langle\hat{N}_1\rangle)\rangle. \tag{11}$$

For this reason, the above statistical mechanical approach is known as the compressibility route. Note that an increase in complexity (number of relevant fields and their associated densities) leads to a rapid growth in the number of these exact results and also related statistical

thermodynamical identities such as Maxwell relations, C_p–C_v relations and Clapeyron equations, [5].

One can also generate statistical mechanical sum rules by scaling the volume and/or shape of the system, thereby generating virial theorems. The leading-order change in the thermodynamic potential that follows from the virial route is given by

$$(\delta\Omega)_{T,\mu} = \left\langle \sum_i \{-k_B T \boldsymbol{\nabla}\cdot\boldsymbol{e}_i + \boldsymbol{e}_i\cdot\boldsymbol{\nabla}_i\Phi\}\right\rangle \tag{12}$$

where

$$\Phi \equiv U + \sum_i v^{ext}(\boldsymbol{r}_i)$$

is the total potential energy and $\boldsymbol{e}$ denotes the displacement field of the deformation. For example, if a planar wall–fluid interface of area $L_x L_y$ lies in the xy-plane, then the interfacial tension (γ) follows from the scaling $\boldsymbol{e} = \epsilon(x, 0, -z)$ where ϵ is an infinitesimal amplitude:

$$\gamma = \frac{1}{L_x L_y}\left\langle \sum_i \left(x_i \frac{\partial\Phi}{\partial x_i} - z_i \frac{\partial\Phi}{\partial z_i}\right)\right\rangle. \tag{13}$$

Of course, the deformation alters more than just the surface area in the xy-plane, but since the ranges of the virial interactions are microscopic it is trivial to remove the unwanted 'line tension' terms, [6], as in fact happens automatically if one sloppily sets all boundaries to infinity, apart from the interface of interest.

Major experimental advances in molecular physics tend to be driven by new techniques that can access a hitherto unexplored or unappreciated thermodynamic field. For example, the surface forces apparatus (SFA) revolutionized the study of fluid solvation within porous media precisely because the key thermodynamic field controlling capillary condensation and adsorption in nano-pores is the dimension of the pore; in the SFA experiment this is a distance between two crossed macroscopic cylindrical walls, [7]. For planar pores, the basic physics is captured by models of the class

$$v^{ext}(z) = \phi(z) + \phi(L - z) \tag{14}$$

where L denotes the separation of the two walls. Here, phase space has been extended by one more dimension (the field L) and the second law (1) picks up an additional term of the form $-f\ \mathrm{d}L$, where the order parameter f is known as the solvation force (or disjoining pressure). The statistical mechanical apparatus sketched above for models of wetting phenomena has also been applied to the solvation of porous media, [1, 8]. The experimental study of wetting phenomena has recently undergone a similar revolution, with the advent of surface chemistry procedures for the formation of self-assembled monolayers (SAMs). The monolayers are firmly attached, usually via silane–glass or thiol–gold bonds, and are designed to present a wide variety of terminal groups to adsorbed fluids. Thus, one can now dial up the desired wetting field strength (ϵ_w) arising from short-range wall–fluid interactions. It is therefore possible to control and study wetting transitions [9] and orientational wetting phenomena [10] in a systematic manner, directly analogous to moving about in statistical mechanical phase space. There are many variations on this versatile set of surface treatment techniques, but one of the key recent developments has been the advent of patterned SAM surfaces. It is already possible to stamp thiol SAMs onto gold-coated substrates, using polymer stamps with detail at the micron level, [11]. Photolithography has also been successful at patterning SAM substrates to at least the micron level. It is clear that technological development will soon push these routine limits into the nano-patterned range, where the patterns will compete directly with molecular interactions. In fact, nano-patterned striped substrates and arrays of circles have recently been

generated via the self-assembly of tri-block copolymer surfactants, [12]. Absorption of fluid within patterned porous media would also present many interesting new phenomena. Perhaps because the ability to manipulate such systems experimentally is so recent, no systematic work has yet been done to describe patterned inhomogeneous fluids. The wetting of striped arrays of hydrophilic and hydrophobic strips has been studied experimentally, [13], a density functional theory has been applied to corrugated surfaces [14, 15], and models of patterned and corrugated surfaces have been studied with simulation and theory, [16–18]. There is also an interesting discussion of the adsorption of drops on macroscopic patterns, constrained by fixed total N, [19]. A mean-field lattice gas model has been shown to generate two-stage capillary condensation within a patterned pore, [20], and a computer simulation technique has been devised to model corrugated SFA experiments, [21].

In the sections below I develop a statistical mechanical framework for patterned inhomogeneous fluids, focusing on extensions of the exact many-body theory outlined above. Firstly, I introduce basic models for patterned and corrugated surfaces, in terms of new thermodynamic fields (section 2). Section 3 discusses the complication that patterning of a fluid interface presents to the virial route, which is directly analogous to the distinction between surface stress and surface tension of a solid surface. Section 4 evaluates specific examples of sum rules that follow from the compressibility route introduced in section 2, applied to fluids adsorbed on planar patterned walls, while section 5 continues the discussion by turning attention to fluids adsorbed within planar patterned pores. Section 6 considers adsorption on corrugated surfaces, emphasizing that corrugation is mathematically related to patterning. The paper concludes (section 7) with a discussion of physical phenomena associated with control over the thermodynamic fields that define the phase space of patterned inhomogeneous fluids.

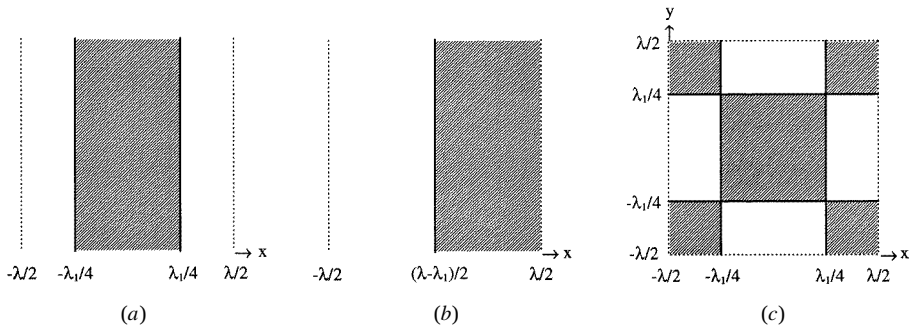

Figure 1. Unit cells for patterned surfaces. Cases (*a*) and (*b*) are alternative choices for generating identical striped patterns, while case (*c*) defines a generalized square lattice. The solid lines denote boundaries between two types of surface–fluid interaction (shaded and unshaded) while the dashed lines indicate periodic boundary conditions. The figure is drawn for the specific case $\lambda = \lambda_1$, but, in general, parameter λ_1 varies the ratio of the coverages, between shaded and unshaded, at fixed overall surface area.

2. Models of patterned and corrugated surfaces

A surface is patterned when its interaction with adsorbed molecules is modulated in some regular manner. The pattern will be defined mathematically by a set of surface lattice vectors, which form the new thermodynamic fields associated with patterning. Hereinafter, I shall use the symbol λ to denote one or more of these patterning fields; i.e. the pattern wavelength. Corrugation is essentially the same phenomenon, but where the dominant effect arises from

modulation of the positions of the surface molecules. The distinction between patterning and corrugation is therefore that in the former only the attractive wall–fluid interactions are patterned, while in the latter the repulsive boundary is modulated as well. The overall shape of the surface (planar, cylindrical etc) is not affected by patterning or corrugation. In this paper, I shall restrict explicit formulae to cases where the wall–fluid interfaces are on average planar. With the above remarks in mind, we can identify two generic classes of models, defined by one-body external fields:

$$v^{ext}(x, y, z) = \zeta(x, y; \lambda)\phi(z) \qquad \text{(patterning)} \tag{15}$$

$$v^{ext}(x, y, z) = \phi(z - \eta\zeta(x, y; \lambda)) \qquad \text{(corrugation).} \tag{16}$$

The pattern function $\zeta(x, y; \lambda)$ is periodic in either x, y or in both directions. One need therefore only define ζ within a unit cell. Figure 1 shows examples of the unit cells for striped patterns and for a generalized square lattice, that I shall employ below for specific discussion. I have chosen to adopt sharp boundaries between the two types of surface area, but note that it is no harder to write down smoothly varying modulation functions. In (15) the modulation ζ would typically be expected to vary between two limits somewhere in the range zero to one; alternatively, one could take $\phi(z)$ to be just the attractive contribution to the unpatterned wall–fluid interaction. Below, when I adopt simple forms with $0 < \zeta < 1$, it is to be understood that the lower limit is $\zeta = 0_+$, so a hard wall boundary is unaffected by the patterning field. In contrast, equation (16) introduces a specific amplitude factor (η) for the corrugation (with ζ chosen to vary between zero and one, or better (section 6), between minus one and one), since the depth of corrugation is obviously a natural thermodynamic field, [18].

The function $\phi(z)$ denotes the external field appropriate to an unpatterned surface lying in the xy-plane. In typical models it might be a short-ranged function such as a square-well interaction, or a long-range power law if dispersion interactions are included. For molecular dynamics simulations, it is common practice to adopt cut and shifted Lennard-Jones models of intermolecular interactions. It is perhaps of interest, then, to note that one could readily pattern such a surface by modulating the position of the cut:

$$v^{ext}(x, y, z) = [\phi(z) - \phi(z_c(x, y; \lambda))]H(z_c(x, y; \lambda) - z) \tag{17}$$

$$z_c(x, y; \lambda) \equiv z_{min} + \zeta(x, y; \lambda)(z_{max} - z_{min}) \tag{18}$$

and H denotes the Heaviside step function.

The parameters λ, η and the phase shift δ (introduced in section 5 below to characterize patterned pores) are the new thermodynamic fields that one must add to phase space to encompass patterned inhomogeneous fluid phenomena. Of course, generalizations come readily to mind, but this is a minimal set for making useful progress. In any given case, one is therefore adding one or more terms to the right-hand side of the second law (1). Since these new fields are present in the external-field contribution to the Hamiltonian only, the order parameters follow directly from the general sum rule, [22],

$$\frac{\partial\Omega}{\partial\nu} = -k_BT \int \mathrm{d}\boldsymbol{r}\, n(\boldsymbol{r}) \frac{\partial}{\partial\nu} \exp\{-v^{ext}(\boldsymbol{r})/k_BT\} \tag{19}$$

where ν denotes any member of the set of additional thermodynamic fields. This result has been written in a form that remains applicable in cases where the external field is not everywhere continuous. In such models the one-body number density $\rho(\boldsymbol{r})$ contains discontinuities, but the function $n(\boldsymbol{r})$ defined by

$$\rho(\boldsymbol{r}) \equiv n(\boldsymbol{r}) \exp\{-v^{ext}(\boldsymbol{r})/k_BT\} \tag{20}$$

is known from diagrammatic theory to always remain continuous ($n(\boldsymbol{r})$ becomes a y-function when one transcribes the wall–fluid system to a two-component mixture in which one of the

components (the wall) is at infinite dilution). Equivalently, this can be stated by saying that in exact theory the one-body direct correlation function must be everywhere continuous. Typical integral equation closures violate this statistical mechanical consistency and thus will not generally satisfy the sum rules derived below. However, weighted density functional theories are by construction free from this problem and thus constitute examples of internally consistent approximations that satisfy the statistical mechanical framework described in this paper, [23]. The compressibility route continues via the next-order result beyond (19), [22],

$$\frac{\partial n(\mathbf{1})}{\partial \nu} = n(\mathbf{1}) \int \mathrm{d}\mathbf{2}\, n(\mathbf{2})[g(\mathbf{1},\mathbf{2}) - 1] \frac{\partial}{\partial \nu} \exp\{-v^{ext}(\mathbf{2})/k_B T\} \tag{21}$$

where $g(\mathbf{1},\mathbf{2})$ denotes the usual pair distribution function.

To conclude this section, I shall define two generic models, to enable the work of the following sections to be carried out explicitly. Many variations on these themes are possible, without requiring any qualitative changes to the derivations. To discuss stripe modulations I will take (see figure 1(*a*))

$$\zeta(x) = \sum_{n=-\infty}^{\infty} H\left(x - n\lambda + \frac{\lambda_1}{4}\right) H\left(n\lambda + \frac{\lambda_1}{4} - x\right) \tag{22}$$

where from now on I will suppress the thermodynamic field arguments of the pattern function ζ. The additional field λ_1 is included to allow for changes in relative coverage, at fixed λ and hence fixed surface area. As a generic model of generalized square patterns I shall choose the class depicted in figure 1(*c*):

$$\zeta(x,y) = \sum_n \sum_m \zeta_{n,m}(x,y) \tag{23}$$

$$\zeta_{n,m}(x,y) = \begin{cases} 1 & \text{if } |x - n\lambda| < \dfrac{\lambda_1}{4} \text{ and } |y - m\lambda| < \dfrac{\lambda_1}{4} \\ 1 & \text{if } \dfrac{\lambda_1}{4} < |x - n\lambda| < \dfrac{\lambda}{2} \text{ and } \dfrac{\lambda_1}{4} < |y - m\lambda| < \dfrac{\lambda}{2} \\ 0 & \text{otherwise.} \end{cases} \tag{24}$$

3. Virial route

The virial route generates sum rules by scaling the dimensions of the system. If the volume remains invariant, then this route yields an expression for the rate of change of surface excess grand potential with change in surface area. For an unpatterned interface, this is just the surface tension, as in equation (13). However, if the deformation alters the pattern (changes λ) then the surface tension itself will vary, even though the adsorbed molecules are fluid. This complication is well known in the study of solid surfaces and solid–melt interfaces, where the left-hand side of (13) is no longer the surface tension (the surface-excess grand potential per surface unit-cell area) but is rather the surface stress, $\sigma = \gamma + A\,\partial\gamma/\partial A$, [24]. Nijmeijer and van Leeuwen have carried out a detailed analysis of a virial route to corrugated wall–fluid models of crystal–fluid interfaces, [25]. These authors make the important observation that virial route expressions such as equation (13) are defined from deformations of the system boundaries (this is perhaps best treated as a containing-field contribution to $v^{ext}(\boldsymbol{r})$) for 'cases in which (the non-containing part of) v^{ext} is not affected by the application of the displacement field'. If the external field were deformed along with the boundaries, then virial route sum rules would not contain a one-body contribution; i.e. Φ would be replaced by U on the right-hand sides of (12) and (13). This is easy to see by noting that the standard derivation procedure involves first altering the system boundaries, then scaling all the position variables to yield a

partition function defined over the original dimensions, with the last step being an expansion of the integrand in terms of the difference between the scaled and original coordinates (the displacement field), [6]. Thus, if v^{ext} was displaced along with the boundaries, then after stage two there would be no change to the one-body terms, and hence no contribution to the change in free energy. The work of reference [25] is restricted to displacements that leave the non-containing external field invariant; I shall refer to this approach applied to patterned substrates as the NvL virial route.

The one-body contributions to virial expressions arise physically from the work done by fluid on the external field, during the deformation. The total work done (on the fluid by the boundary walls and by the fluid on the boundary walls) is zero, since the total equilibrium free energy is stationary with respect to volume fluctuations at fixed external field, [26]. Thus, the displacement must be applied to the containing field in order to separate out the quantity of interest; i.e. to exclude the work done by the fluid on the containing walls. In contrast, one would not want to deform the substrate field normal to a planar wall, $\phi(z)$, while the L_z-dimension is scaled to fix the total volume, since this would represent an unphysical compression of the attractive wall–fluid interaction as the volume is decreased. However, the surface stress sum rules, described above by analogy to a crystal–fluid interface, do require one to displace the pattern/corrugation field during stretching or compression of the interface. I shall refer to this approach as the natural virial route, when applied to a patterned interface. Thus, in the natural route, there are no one-body contributions arising from work done by fluid against the $\zeta(x, y)$ pattern field, and note also that the surface always contains an integer number of surface unit cells. In contrast, the NvL route corresponds to growing an infinitesimal amount of additional interface, without scaling the pattern field, and thus inevitably generates expressions that reflect an ambiguity as to which part of the periodic pattern is adjacent to the newly grown interface; these results must therefore be averaged over the growth of an entire additional wavelength. I will return to this subtle issue below, but first let me evaluate expressions from the natural virial route, to act as explicit examples.

For striped patterns one can use the natural route to generate virial expressions for both the surface stress and the surface tension. Consider, for example, fluid adsorbed on the striped pattern depicted in figure 1(a). If the system (including the pattern) is stretched along the axis normal to the pattern (the x-axis) then the pattern is deformed and the resulting virial theorem will yield the surface stress. In contrast, if the displacement is along the direction of the stripes only, then there is no alteration to the stripe wavelength (note that a stripe is not allowed to be patterned or corrugated along its defining direction) and so the restoring force for this distortion is purely surface tension. To carry out these procedures explicitly, one applies the same derivation that led to (13), but with the additional feature that the stripe wavelength is deformed along with the surface dimension in the direction normal to the stripes:

$$\gamma(\lambda) + \lambda\frac{\partial\gamma}{\partial\lambda} = \frac{1}{L_x L_y}\left\langle \sum_i \left(x_i \frac{\partial U}{\partial x_i} - z_i \frac{\partial \Phi}{\partial z_i} \right) \right\rangle \tag{25}$$

while the deformation $\boldsymbol{e} = \epsilon(0, y, -z)$ yields

$$\gamma(\lambda) = \frac{1}{L_x L_y}\left\langle \sum_i \left(y_i \frac{\partial U}{\partial y_i} - z_i \frac{\partial \Phi}{\partial z_i} \right) \right\rangle \tag{26}$$

so from combining these expressions we also have

$$\lambda\frac{\partial\gamma}{\partial\lambda} = \frac{1}{L_x L_y}\left\langle \sum_i \left(x_i \frac{\partial U}{\partial x_i} - y_i \frac{\partial U}{\partial y_i} \right) \right\rangle. \tag{27}$$

For a simple pair potential model ($U = \sum\sum_{i<j} u(r_{ij})$), in the presence of the external field

(15, 22), the above results reduce to

$$\gamma(\lambda) = \frac{1}{L_x L_y}\left\{\int \mathrm{d}\mathbf{1}\int \mathrm{d}\mathbf{2}\ \rho(\mathbf{1})\rho(\mathbf{2})g(\mathbf{1},\mathbf{2})\left(\frac{y_{12}^2 - z_{12}^2}{2r_{12}}\right)u'(r_{12}) - \int \mathrm{d}\mathbf{1}\ \rho(\mathbf{1})\zeta(x_1)z_1\phi'(z_1)\right\} \tag{28}$$

$$\lambda\frac{\partial\gamma}{\partial\lambda} = \frac{1}{L_x L_y}\left\{\int \mathrm{d}\mathbf{1}\int \mathrm{d}\mathbf{2}\ \rho(\mathbf{1})\rho(\mathbf{2})g(\mathbf{1},\mathbf{2})\left(\frac{x_{12}^2 - y_{12}^2}{2r_{12}}\right)u'(r_{12})\right\}. \tag{29}$$

Similarly, the symmetric surface displacement $\boldsymbol{e} = \epsilon(x, y, -2z)$ applied to the generalized square pattern of figure 1(c) yields the sum rule

$$\gamma(\lambda) + \frac{\lambda}{2}\frac{\partial\gamma}{\partial\lambda} = \frac{1}{L_x L_y}\left\{\int \mathrm{d}\mathbf{1}\int \mathrm{d}\mathbf{2}\ \rho(\mathbf{1})\rho(\mathbf{2})g(\mathbf{1},\mathbf{2})\left(\frac{x_{12}^2 + y_{12}^2 - 2z_{12}^2}{4r_{12}}\right)u'(r_{12}) - \int \mathrm{d}\mathbf{1}\ \rho(\mathbf{1})\zeta(x_1, y_1)z_1\phi'(z_1)\right\}. \tag{30}$$

The final terms in (28) and (30) are one-body contributions to the disjoining pressure (as noted above, these arise from the work done on the external field by the fluid), but the analogous term in (29) is missing because the pattern field $\zeta(x)$ has been scaled along with the surface dimensions. Similarly, the right-hand side of (30) contains no one-body terms involving derivatives of the pattern function $\zeta(x, y)$.

To appreciate the significance of this last point, let us evaluate the term absent from the right-hand side of (29); i.e. the one-body surface stress contribution that arises in the NvL route; with $\zeta(x)$ defined by (22):

$$\frac{1}{L_x L_y}\int \mathrm{d}\boldsymbol{r}\ \rho(\boldsymbol{r})x\zeta'(x)\phi(z) = -\frac{k_B T}{L_x L_y}\int \mathrm{d}\boldsymbol{r}\ n(\boldsymbol{r})x\ \frac{\partial}{\partial x}\exp\{-\zeta(x)\phi(z)/k_B T\} \tag{31}$$

$$= -\frac{k_B T}{L_x}\int_0^\infty \mathrm{d}z\ n_w(z)[\exp(-\phi(z)/k_B T) - 1] \times \sum_n\left\{\left(n\lambda - \frac{\lambda_1}{4}\right) - \left(n\lambda + \frac{\lambda_1}{4}\right)\right\} \tag{32}$$

$$= \frac{k_B T\lambda_1}{2\lambda}\int_0^\infty \mathrm{d}z\ \Delta\rho_w(z). \tag{33}$$

Here, I have introduced the subscript w to denote a quantity evaluated on the side 'walls' of the pattern (i.e. at $x = \pm\lambda_1/4$ in figure 1(a)), with $\Delta\rho_w(z)$ denoting the discontinuous jump in density across these pattern walls. Now shift the pattern in figure 1(a) by the amount $\lambda/2$ and evaluate the same integral; it changes from equation (33) to

$$-k_B T\left(1 - \frac{\lambda_1}{2\lambda}\right)\int_0^\infty \mathrm{d}z\ \Delta\rho_w(z). \tag{34}$$

The unphysical nature of this quantity has been noted before, [27, 28]. The lack of uniqueness arises because the process of growing an infinitesimal amount of additional surface, while keeping the pattern field invariant, depends on which part of the pattern is being newly exposed. Nijmeijer and van Leeuwen, [25], take the view that the NvL route expressions should be averaged over such shifts (namely, over displacement of the pattern within the periodically repeated unit cell, between the above two limits). That is, the surface tension is well defined by processes that grow integer numbers of additional surface unit cells. In fact, for my example the integral (31) only ever evaluates to either of the above answers and the NvL route average is easily seen to be zero.

Up to now, my discussion has tacitly assumed that the natural virial route and the NvL method are two alternative approaches to obtaining well-defined statistical mechanical sum rules, provided the latter is averaged over displacements of the pattern within the periodic unit cell. However, it appears from (29) and (30) that they disagree over the presence or absence of a fluid–fluid contribution to the surface stress. Nijmeijer and van Leeuwen state 'the (fluid–fluid contribution) does not depend on the location of the (pattern with respect to the containing walls)' so the 'integral over different locations of the (pattern with respect to the walls) is therefore trivial.' This would imply that the left-hand side of (30) is the surface tension γ, rather than the surface stress as I have stated. However, the two virial routes, natural and NvL, correspond to different physical processes and should in fact involve different values for the work done. Note, in particular, that the natural route generates a change in the pattern wavelength, which in turn should affect the fluid–fluid contribution to the interfacial free energy; consider for example an extreme case where the size of the attractive region of the pattern is crossing over from a regime in which one fluid molecule prefers to sit on each site to the situation in which two will sit on each site. The result (29) is an example of a fluid–fluid contribution to surface stress that is perfectly physical and yet it seems that it would need to be identically zero if the above-mentioned average required in the NvL route is as trivial as previously stated. Other workers have noted that expressions of the class (30) must define the surface stress (as distinct from surface tension) in models of crystal–fluid interfaces, [24, 29]. A density functional calculation by Tarazona and Velasco, [15], appears to confirm that even when the crystal surface is replaced by a corrugated wall, there remains a significant difference between surface tension and surface stress. This issue is of some importance to computer simulation studies of patterned inhomogeneous fluids, that aim to make use of the virial route, [28]. Clearly, simulators will need to make a careful study of the above discussion and that contained in references [15, 24, 25, 29]; for example, to decide precisely what the left-hand side of (30) should be physically. If (30) is correct as I have derived it, then a procedure analogous to that developed by Tarazona and Velasco [15] is needed to separate out the surface tension contribution. It is therefore with some relief that I now turn attention to the compressibility route for patterned inhomogeneous fluids, which is conceptually much simpler because one only considers processes for which the overall system dimensions remain invariant; directly opposite to an NvL virial route procedure.

4. Compressibility sum rules for planar patterned walls

Continuing discussion of the basic model of a stripe pattern, figure 1(*a*), with the pattern field defined by equation (22), I shall now turn attention to variation of λ_1 at fixed λ. This process takes place at fixed volume, surface area and overall dimensions of the surface unit cell. Physically, this represents growth of one region of the stripe pattern at the expense of its opposite. Sum rule (19) yields the rate of change of surface tension, as the relative coverage is varied:

$$\frac{\partial\gamma}{\partial\lambda_1} = -\frac{k_BT}{4L_xL_y}\int \mathrm{d}\boldsymbol{r}\; n(\boldsymbol{r})\,\frac{\partial}{\partial\lambda_1/4}\exp\{-\zeta(x)\phi(z)/k_BT\} \tag{35}$$

$$= -\frac{k_BT}{2\lambda}\int_0^\infty \mathrm{d}z\; n_w(z)[\exp(-\phi(z)/k_BT) - 1] \tag{36}$$

$$\equiv -\frac{k_BT}{2\lambda}\int_0^\infty \mathrm{d}z\; \Delta\rho_w(z). \tag{37}$$

Here, I have used notation identical to that introduced in (33), but note that the evaluation of the above integral does not depend on the origin of the pattern within the periodically repeated

unit cell, in contrast to the quantity (31). This of course reflects the different nature of the physical processes involved. Continuing the differentiation leads to a sum rule for what one might entitle the coverage compressibility; i.e. $\partial^2\gamma/\partial\lambda_1^2$. However, the choice of coordinates depicted in figure 1(a) is not a helpful one for this purpose, because sum rule (21) does not yield the change in the pattern wall density, n_w, if the wall itself is moving with variation of λ_1. This problem is easily avoided by switching to an equivalent choice of surface unit cell depicted in figure 1(b), to evaluate the change in n_w positioned at fixed $x = \lambda/2$, while the other pattern wall is moved:

$$\frac{\partial n_w(z_1)}{\partial\lambda_1} = \frac{n_w(z_1)}{2}\int \mathrm{d}\mathbf{2}\; n(\mathbf{2})[g(\mathbf{1},\mathbf{2})-1]\,\frac{\partial}{\partial\lambda_1/2}\exp\{-\zeta(x_2)\phi(z_2)/k_BT\} \tag{38}$$

$$= \frac{n_w(z_1)}{2}\int_0^\infty \mathrm{d}z_2\; n_w(z_2)[\exp(-\phi(z_2)/k_BT)-1]$$
$$\times \sum_n \int_{-\infty}^{\infty} \mathrm{d}y_{12}\,[g(x_{12}=n\lambda-\lambda_1/2,\, y_{12}, z_1, z_2; x_1=\lambda/2)-1]. \tag{39}$$

Substituting this result into the derivative of (37) and then switching back to the coordinates defined in figure 1(a) yields

$$\frac{\partial^2\gamma}{\partial\lambda_1^2} = -\frac{k_BT}{4\lambda}\int_0^\infty \mathrm{d}z_1\;\Delta\rho_w(z_1)\int_0^\infty \mathrm{d}z_2\;\Delta\rho_w(z_2)$$
$$\times \sum_n \int_{-\infty}^{\infty} \mathrm{d}y_{12}\,[g(x_{12}=n\lambda-\lambda_1/2,\, y_{12}, z_1, z_2; x_1=\lambda_1/4)-1]. \tag{40}$$

Note that the sum only runs over pair correlations between all left-hand pattern walls with one right-hand pattern wall, or vice versa. This result has a simple physical interpretation. For example, in the limit where the width of the shaded regions becomes macroscopic, while the unshaded regions remain microscopic, then only one term in the sum is relevant. This term describes correlations between either side of an unshaded strip, directly analogous to the correlations that determine the solvation compressibility ,$-\partial f/\partial L$, for a solvated planar pore of the class (14); [1, 8]. If the system is in a region of phase space such that liquid is only adsorbed on the shaded strips, then by reducing the width of the unshaded strips one approaches a transition to wetting of the entire substrate. If this transition were continuous, then the correlation length for pair correlations across the unshaded strips, controlling the range of the integrand in (40), would diverge. If the transition were first order, then nucleation of a liquid path across unshaded strips would happen before surface critical phenomena could take place. Naturally, the full sum on the right-hand side of (40) enables cooperative effects between the wetting of distinct stripes to occur.

The same analysis can be applied to the generalized square pattern depicted in figure 1(c); i.e. equations (23), (24). Variation of λ_1 alters the relative coverage of shaded to unshaded surface and at the same time alters the shape of the unshaded surface cells. Of course, any type of pattern will be defined by a set of parameters analogous to λ_1 and thus the qualitative nature of the coverage compressibility route remains the same. The leading-order sum rule maintains a simple form:

$$\frac{\partial\gamma}{\partial\lambda_1} = -\frac{k_BT}{4\lambda^2}\int_0^\infty \mathrm{d}z\;\left\{\oint_{c_e}\mathrm{d}\ell - \oint_{c_s}\mathrm{d}\ell\right\}\Delta\rho_w(x,y,z) \tag{41}$$

where the curve c_e denotes the boundary of the unit-cell shaded square that expands as λ_1 increases and the other line integral goes around the boundary of the shaded square that shrinks; note that each unit cell contains two shaded squares and two unshaded rectangles.

5. Solvation of patterned porous media

In this section I consider the generalization of the basic model of a planar pore, equation (14), to situations where the two pore surfaces are patterned with identical unit cells, except for a phase shift δ. Taking stripe patterns as the specific example, I thus define

$$v^{ext}(x, z) = \zeta(x - \delta)\phi(z) + \zeta(x)\phi(L - z) \tag{42}$$

where $0 \leqslant \delta \leqslant \lambda/2$. This introduces a new thermodynamic field δ, whose variation corresponds to a shearing motion. I shall only consider this process carried out at equilibrium. Let me restrict explicit results to cases where the two walls do not directly interact; i.e. L is greater than the range of the surface–surface interaction, so only the surface–fluid interactions play a direct role. Then, continuing to adopt (22) as the basic model of a striped pattern, the change in interfacial free energy is readily evaluated as

$$\frac{\partial\gamma}{\partial\delta} = -\frac{k_BT}{2L_xL_y}\int \mathrm{d}\boldsymbol{r}\, n(\boldsymbol{r}) \exp\{-\zeta(x)\phi(L - z)/k_BT\}\, \frac{\partial}{\partial\delta} \exp\{-\zeta(x - \delta)\phi(z)/k_BT\} \tag{43}$$

$$= \frac{k_BT}{2\lambda}\int_0^L \mathrm{d}z\ [\Delta\rho_w(z; x = \delta - \lambda_1/4) - \Delta\rho_w(z; x = \delta + \lambda_1/4)]\,. \tag{44}$$

Note that the surface area has now doubled ($A = 2L_xL_y$) and that if the range of $\phi(z)$ is less than L then the upper limit on the integral in (44) is reduced (the pattern wall densities belong to the bottom surface stripes only). Sum rule (44) displays the periodic symmetry inherent in (42); i.e. $\partial\gamma/\partial\delta$ is zero at $\delta = 0$ or $\lambda/2$. Thus, at these limits the surface tension is a maximum and a minimum, respectively, or vice versa. The right-hand side of (44) also highlights those situations in which the physical effects of a phase shift are maximized—for example, when the pore is partially filled such that liquid bridges form between the shaded strips only, or when the pore is largely solvated except for bubbles attached to the unshaded strips. In these cases the rate of change of surface tension with phase shift is significant for phase shifts in the vicinity of $\lambda/4$, given that L is sufficiently small to allow for fluid-mediated correlations between the pore surfaces, because the difference between the local environments of the pattern walls at $x = \delta \pm \lambda_1/4$ is maximized.

The compressibility route hierarchy is readily continued, but I shall avoid the notation needed to generate explicit results. Clearly, one only need adapt the method used to generate sum rule (40); for example, note that it is important to calculate the rate of change of $n_w(z)$ on the surface that is not being moved during alteration of the phase shift, in order to make immediate use of (21). The result is very similar to a set of terms of the form (40), but now each double integral is over a product of a pair of pattern wall densities that originate from opposite surfaces (the relevant correlations span the pore surfaces). The compressibility $\partial^2\gamma/\partial\delta^2$ is obviously of interest when liquid or vapour bridges connect the two surfaces, since then there exist strong pair correlations along the bridge edges.

6. Corrugated inhomogeneous fluids

A corrugated wall–fluid interface is a class of patterned inhomogeneous fluid, but where the dominant physical effect arises from modulation of the repulsive wall–fluid interaction. Accordingly, to discuss the basic physics of corrugation I need only consider model (16) in the limit where $\phi(z)$ is a hard-wall potential ($\phi_{HW}(z) = 0$ for $z > 0$, ∞ if $z < 0$). Again, let me concentrate on stripe patterns of the class (22), but now with

$$v^{ext}(x, z) = \phi_{HW}(z - \eta\zeta(x)). \tag{45}$$

Applying (19) yet again to the pattern depicted in figure 1(*a*),

$$\frac{\partial\gamma}{\partial\lambda_1} = -\frac{k_BT}{4L_xL_y}\int \mathrm{d}\boldsymbol{r}\; n(\boldsymbol{r})\,\frac{\partial}{\partial\lambda_1/4}\exp\{-\phi_{HW}(z-\eta\zeta(x))/k_BT\} \tag{46}$$

$$= \frac{\eta k_BT}{4\lambda}\int_{-\lambda/2}^{\lambda/2}\mathrm{d}x\;\rho_w(x)\frac{\partial\zeta(x)}{\partial\lambda_1/4} \tag{47}$$

where $\rho_w(x)$ denotes the fluid density at the surface of the corrugated hard wall. At first sight, equation (22) looks problematic for use with (47), but this is easily avoided by taking the limit of very steep linear side walls:

$$\zeta(x) = \frac{1}{2} \pm \frac{1}{\epsilon}\left(x \pm \frac{\lambda_1}{4}\right) \tag{48}$$

for $0 < \zeta < 1$ and ϵ arbitrarily small but positive. Outside these small ranges of x, the integrand of (47) evaluates to zero because ζ is fixed at zero or unity. Along the side walls, $\partial\zeta(x)/\partial(\lambda_1/4)$ is $1/\epsilon$, and one can use this to change the integration variable from x to z; i.e. at $z = \eta\zeta$ we have $\mathrm{d}z = \pm(\eta/\epsilon)\,\mathrm{d}x$ and hence

$$\frac{\partial\gamma}{\partial\lambda_1} = \frac{k_BT}{2\lambda}\int_0^\eta \mathrm{d}z\;\rho_w(z;\,x=\lambda_1/4). \tag{49}$$

The above process changes the relative corrugation widths of protrusions and recessions, at fixed amplitude η, and thus alters the volume (V_f) available to the centres of fluid particles. Accordingly, it must be possible to view the change in free energy $A\,\partial\gamma$ as a $-\bar{p}\,\partial V_f$ term with $\bar{p}$ an effective pressure. Since $\partial V_f/\partial\lambda_1 = -\eta A/2\lambda$, sum rule (49) identifies $\bar{p}$ with

$$\bar{p} \equiv \frac{k_BT}{\eta}\int_0^\eta \mathrm{d}z\;\rho_w(z;\,x=\lambda_1/4) \tag{50}$$

as one would anticipate.

The correspondence between (49) and (37) is to be expected, because hard-wall corrugation is actually a special case of patterning for which the shaded stripe is an infinitely repulsive field (rather than an attractive one); i.e. $\Delta\rho_w(z) = -\rho_w(z)$. I can therefore make use of this mathematical translation to write down by inspection the corrugation compressibility sum rule:

$$\frac{\partial^2\gamma}{\partial\lambda_1^2} = -\frac{k_BT}{4\lambda}\int_0^\eta \mathrm{d}z_1\;\rho_w(z_1)\int_0^\eta \mathrm{d}z_2\;\rho_w(z_2)$$

$$\times\sum_n\int_{-\infty}^{\infty}\mathrm{d}y_{12}\,[g(x_{12}=n\lambda-\lambda_1/2,\,y_{12},\,z_1,\,z_2;\,x_1=\lambda_1/4)-1]. \tag{51}$$

In the limit $\eta = \infty$ the intermediate step, analogous to (39), can be checked against the compressibility for solvation of a planar hard pore of width $L = \lambda - \lambda_1/2$, whose walls lie parallel to the yz-plane, [1, 8],

$$\frac{\partial\rho_w}{\partial L} = \rho_w^2\int_{-\infty}^{\infty}\mathrm{d}y_{12}\int_{-\infty}^{\infty}\mathrm{d}z_{12}\,[g(x_1=0,\,x_2=L,\,y_{12},\,z_{12})-1]. \tag{52}$$

The same mathematical translation is equally applicable to the hard-wall corrugation limit of the generalized square pattern in figure 1(*c*); cf. equation (41) and note the obvious generalization of (50).

The shearing of solvated corrugated pores can be treated as a class of patterning, in the same way, but note how much more significant has become my restriction to cases where there is no direct interaction between the pore surfaces. For a pore–fluid field of the class

$$v^{ext}(x,z) = \phi_{HW}(z-\eta\zeta(x-\delta)) + \phi_{HW}(L-z-\eta\zeta(x)) \tag{53}$$

with $\zeta(x)$ defined by (22), sum rule (44) translates to

$$\frac{\partial\gamma}{\partial\delta} = -\frac{k_BT}{2\lambda}\int_0^\eta \mathrm{d}z\ [\rho_w(z; x = \delta - \lambda_1/4) - \rho_w(z; x = \delta + \lambda_1/4)] \tag{54}$$

$$= \left(\frac{\eta}{2\lambda}\right)\Delta\bar{p} \tag{55}$$

where $\Delta\bar{p}$ denotes a difference, from right to left of a protrusion, of two terms of the type (50). Sum rule (54) is of course a periodic function of δ, for the same reasons of symmetry as apply to (44). Version (55) shows that the order parameter $\partial\gamma/\partial\delta$ is proportional to a transverse pressure difference, arising from an imbalance of collisions of the fluid particles with opposite sides of a protrusion. An extreme example of such an imbalance arises, for $\delta \simeq \lambda/4$, when L is sufficiently small that repulsive wall–fluid interactions prevent particles from occupying any region of the pore not simultaneously bounded by recessed (unshaded) regions. Note that all of the sum rules that I have discussed apply at fixed temperature and chemical potential, so large values of the pore order parameters typically denote regions of phase space where small changes in the conjugate thermodynamic field lead to dramatic filling or emptying of the porous media.

The new thermodynamic field associated with corrugation is the amplitude η. Returning to the corrugated surface–fluid interface defined by (45), I can once again invoke (19), to obtain the conjugate order parameter:

$$\frac{\partial\gamma}{\partial\eta} = -\frac{k_BT}{L_xL_y}\int \mathrm{d}\boldsymbol{r}\ n(\boldsymbol{r})\ \frac{\partial}{\partial\eta}\exp\{-\phi_{HW}(z - \eta\zeta(x))/k_BT\} \tag{56}$$

$$= \frac{k_BT}{\lambda}\int_{-\lambda/2}^{\lambda/2}\mathrm{d}x\ \rho_w(x)\zeta(x). \tag{57}$$

If (22) is substituted for $\zeta(x)$, then (57) reduces to

$$\frac{\partial\gamma}{\partial\eta} = \frac{k_BT}{\lambda}\int_{-\lambda_1/4}^{\lambda_1/4}\mathrm{d}x\ \rho_w(x) \equiv \bar{p}\left(\frac{\lambda_1}{2\lambda}\right) \tag{58}$$

which is obviously a $-\bar{p}\,\partial V_f$ term (this $\bar{p}$ belongs to the top wall of a protrusion, rather than the side walls as in (50)), reflecting the fact that the volume available to the fluid particles is decreased as η increases. In this sense, it is perhaps inappropriate to use the stripe pattern (22) to discuss the corrugation field η. If instead, $\zeta(x)$ is redefined to oscillate about zero, then one can readily arrange that the free volume remains invariant as η is varied; for example, ζ switching between -1 and 1 is appropriate to the case $\lambda_1 = \lambda$. This choice alters sum rule (58), such that the right-hand side becomes a difference between two such terms, corresponding to an effective pressure difference between the top and bottom regions of the corrugated surface.

The previous remark shows that grasping the physical significance of the above sum rules and their generalizations demands a clear appreciation of the meaning of the terms surface, hard wall, and the associated concept of free volume. The statistical mechanics described in this paper is based exclusively on using an external field to represent surface–fluid interactions. Thus, the terms surface and hard wall refer to a surface–fluid boundary, not the surface that would be visible from an actual molecular model. For example, if the fluid molecules are spheres, the phrase 'corrugated hard wall' denotes a periodic boundary beyond which the centres of the fluid spheres are excluded. Thus, V, which denotes $L_xL_yL_z$, is not equivalent to V_f, the free volume available to spheres. Herein lies the physical reason for $A\,\partial\gamma$ sum rules often possessing the character of a $-p\,\partial V$ term. Similar comments apply to corrugated pores; for example, it is only where the hard-wall patterns overlap that the centres of fluid spheres are prevented from solvating regions between the protrusions.

7. Discussion

In this paper I have relied on specific generic examples to illustrate the statistical mechanics of patterned inhomogeneous fluids. So, how general is the physics that I have described? Firstly, note that nowhere, apart from references to pair potential fluid models in some aspects of the virial route alone, have I needed to specify the fluid–fluid Hamiltonian U. The external fields (15) and (16), and their applications to porous media, are already quite general. This applies both to the substrate–fluid interaction ϕ and the pattern field ζ. Varying the specific choices that I have often made for these functions, in order to generate explicit results, will not invalidate any of the sum rule methods that I have applied.

There are, however, some qualitative generalizations that require an expanded notation and additional thermodynamic fields. To discuss patterned inhomogeneous fluid mixtures requires a different v^{ext} for each species of the mixture. Control over the relative attractive surface–fluid interactions, between different species, yields sum rules for patterning phenomena such as periodic competitive adsorption and periodic partitioning within porous media. Differences in the repulsive interactions may often be equally important, especially with corrugated surfaces and pores. Here, one must note carefully (cf. my comments at the end of section 6) that each species–surface repulsive range defines a different excluded volume (one for each species). Thus, corrugated fluid mixtures display patterns defined by a set of corrugated walls, some of which must be allowed to overlap to describe situations in which the recessions exclude large particles. This is analogous to reducing a pore width until it can no longer accommodate the largest diameter species. Similar remarks apply to generalizations needed to account for the orientational degrees of freedom of adsorbed non-spherical molecules. Typically, one describes a surface–molecule interaction in terms of the position of the centre of the molecule and its orientation with respect to a surface normal. Thus, for example, planar rods can approach a hard wall closer than homeotropic rods. Corrugation will obviously align rod- and disc-shaped molecules; e.g. in extreme cases corrugated surfaces only allow penetration by homeotropic rods. The entire statistical mechanical structure described above carries over to these more complex situations, provided care is taken in defining a suitable surface–fluid interaction. Of course, the greatly expanded regime of relevant physics is associated with an ever increasing set of relevant thermodynamic fields. As long as these new fields are incorporated solely as parameters within a generalized one-body interaction (v^{ext}), then sum rules (19) and (21) can be directly applied. The compressibility route therefore remains extremely accessible, regardless of the complexity.

What then of the myriad physical phenomena available to those who learn to control the new thermodynamic fields associated with patterning? For example, imagine a surface chemistry obtained from self-assembled monolayers of robust optically active switches (cf. azobenzenes). Then, given a few more years of development, one could use laser scanning to activate reversible pattern switching, which if combined with scanning microscope technology would be extendible into the nano-pattern regime of particular interest to statistical mechanics. Pore selectivity, between liquid and vapour or between different species of fluid, could be controlled, as in sum rules (44), (55). The wetting of patterned surfaces could be dramatically varied by sitting close to surface transitions controlled by the geometry of the pattern; cf. sum rules (37), (41), (49), (58). Perhaps the most interesting regime is the near nano-pattern wavelength, where the atomic corrugation of solid surfaces can be ignored (averaged), but the relative adsorption of liquid and vapour or between different numbers of molecular layers is readily controlled. Here, one will observe phenomena such as multistage adsorption isotherms and multistage and re-entrant capillary condensation and pore selectivity. Note also that fluctuation phenomena will sometimes play a crucial role. In general, one expects

patterning to lead to enhanced fluctuations, since the price paid in energy for solvating non-wetting regions will typically be minimized with rough interfaces or film thicknesses. Sum rules (40), (51) highlight some of this physics, but quite deep issues do arise. In particular, the adsorption of fluid on a patterned surface can involve more than just the symmetry of the surface–fluid interaction, even in equilibrium. That is, the dominant symmetry may sometimes be merely commensurate with the underlying pattern; e.g. if every second unshaded stripe were solvated along with the shaded ones.

Finally, it is worth stressing the point noted in section 2, that weighted density functional theories are fully consistent with both the compressibility route, via identical derivations [30], and also the virial route, via mechanical equilibrium expressed in terms of wall-density sum rules [23]. Thus, there are three potentially important uses of the sum rule analyses presented in this paper:

(i) evaluation by approximate density functionals, both to confirm the validity of the density functional numerical procedures and to describe the phase space under investigation,
(ii) for similar use with computer simulation procedures and
(iii) deriving limiting or approximate analytical solutions.

References

[1] Henderson J R 1992 *Fundamentals of Inhomogeneous Fluids* ed D Henderson (New York: Dekker) p 23
[2] Allen M P and Tildesley D J 1987 *Computer Simulation of Liquids* (Oxford) §11.5
[3] Mermin N D 1965 *Phys. Rev.* A **137** 1441
[4] Griffiths R B and Wheeler J C 1970 *Phys. Rev.* A **2** 1047
[5] Evans R and Marini Bettolo Marconi U 1987 *J. Chem. Phys.* **86** 7138
[6] Lekner J and Henderson J R 1977 *Mol. Phys.* **34** 333
[7] Israelachvili J N 1992 *Intermolecular and Surfaces Forces* (New York: Academic)
[8] Henderson J R 1986 *Mol. Phys.* **59** 89
[9] Franck C 1992 *Fundamentals of Inhomogeneous Fluids* ed D Henderson (New York: Dekker) p 277
[10] Evans S D, Allinson H, Boden N and Henderson J R 1996 *Faraday Discuss.* **104** 37
[11] Kumar A and Whitesides G M 1993 *Appl. Phys. Lett.* **63** 2002
[12] Kim G and Libera M 1998 *Macromolecules* **31** 2569
[13] Drelich J, Wilbur J L, Miller J D and Whitesides G M 1996 *Langmuir* **12** 1913
[14] Velasco E and Tarazona P 1989 *J. Chem. Phys.* **91** 7916
[15] Henderson J R, Tarazona P, van Swol F and Velasco E 1992 *J. Chem. Phys.* **96** 4633
[16] Urban D, Topolski K and De Coninck J 1996 *Phys. Rev. Lett.* **76** 4388
[17] Swain P S and Parry A O 1997 *J. Phys. A: Math. Gen.* **30** 4597
[18] Patrykiejew A, Sokolowski S, Zientarski T and Binder K 1998 *J. Chem. Phys.* **108** 5068
[19] Lenz P and Lipowsky R 1998 *Phys. Rev. Lett.* **80** 1920
[20] Rocken P and Tarazona P 1996 *J. Chem. Phys.* **105** 2034
[21] Douglas Frink L J and van Swol F 1998 *J. Chem. Phys.* **108** 5588
[22] Van Swol F and Henderson J R 1986 *J. Chem. Soc. Faraday Trans.* II **82** 1685
[23] Van Swol F and Henderson J R 1989 *Phys. Rev.* A **40** 2567
[24] Shuttleworth R 1950 *Proc. Phys. Soc.* A **63** 444
Broughton J Q and Gilmer G H 1986 *J. Chem. Phys* **84** 5759
[25] Nijmeijer M J P and van Leeuwen J M J 1990 *J. Phys. A: Math. Gen.* **23** 4211
[26] Schofield P and Henderson J R 1982 *Proc. R. Soc.* A **379** 231
[27] Nijmeijer M J P and Bruin C 1996 *J. Chem. Phys.* **105** 4889
[28] Harris J G 1996 *J. Chem. Phys.* **105** 4891
[29] Van Swol F 1988 *Phys. Rev. Lett.* **60** 239
[30] See e.g. Evans R 1979 *Adv. Phys.* **28** 143